




Reduced Uterine Tissue Damage during *Chlamydia muridarum* Infection in TREM-1,3-Deficient Mice

Bryan E. McQueen,^{a,b} Avinash Kollipara,^a Clare E. Gyorke,^{a,b} Charles W. Andrews, Jr.,^d Ashley Ezzell,^c Toni Darville,^{a,b}
 Uma M. Nagarajan^{a,b}

^aDepartment of Pediatrics, University of North Carolina, Chapel Hill, North Carolina, USA

^bDepartment of Microbiology and Immunology, University of North Carolina, Chapel Hill, North Carolina, USA

^cDepartment of Cell Biology and Physiology, University of North Carolina, Chapel Hill, North Carolina, USA

^dDepartment of Pathology and Immunology, Baylor College of Medicine, Houston, Texas, USA

ABSTRACT Genital infections with *Chlamydia trachomatis* can lead to uterine and oviduct tissue damage in the female reproductive tract. Neutrophils are strongly associated with tissue damage during chlamydial infection, while an adaptive CD4 T cell response is necessary to combat infection. Activation of triggering receptor expressed on myeloid cells-1 (TREM-1) on neutrophils has previously been shown to induce and/or enhance degranulation synergistically with Toll-like receptor (TLR) signaling. Additionally, TREM-1 can promote neutrophil transepithelial migration. In this study, we sought to determine the contribution of TREM-1,3 to immunopathology in the female mouse genital tract during *Chlamydia muridarum* infection. Relative to control mice, *trem1,3^{-/-}* mice had no difference in chlamydial burden or duration of lower-genital-tract infection. We also observed a similar incidence of hydrosalpinx 45 days postinfection in *trem1,3^{-/-}* compared to wild-type (WT) mice. However, compared to WT mice, *trem1,3^{-/-}* mice developed significantly fewer hydrometra in uterine horns. Early in infection, *trem1,3^{-/-}* mice displayed a notable decrease in the number of uterine glands containing polymorphonuclear cells and uterine horn lumens had fewer neutrophils, with increased granulocyte colony-stimulating factor (G-CSF). *trem1,3^{-/-}* mice also had reduced erosion of the luminal epithelium. These data indicate that TREM-1,3 contributes to transepithelial neutrophil migration in the uterus and uterine glands, promoting the occurrence of hydrometra in infected mice.

KEYWORDS *Chlamydia*, TREM-1, neutrophils, PMNs, hydrosalpinx, hydrometra, *Chlamydia trachomatis*, genital disease, mouse

The most common sexually transmitted bacterial infection in women is caused by *Chlamydia trachomatis* (1). Infection is often asymptomatic and goes undetected, leading to ongoing inflammation that causes pelvic inflammatory disease with sequelae such as chronic pelvic pain, ectopic pregnancy, and/or infertility (2–4). Excessive neutrophil recruitment in the upper genital tract during chlamydial infection contributes to long-term damage (5–7). It is well established that in mucosal tissues, neutrophils can promote epithelial damage and disrupt barrier function when they cross from the basal side of the epithelium into the lumen (6, 8–11). Therefore, identification of the precise mechanisms that induce neutrophil recruitment, transepithelial migration (TeM), and activation in the genital mucosa could reveal potential therapeutic targets to alleviate sequelae during chlamydial infections.

Neutrophils express G-protein-coupled, Fc, adhesion, cytokine, and pattern recognition receptors on their surfaces, which are activated during pathogenic infections (reviewed in reference 12). However, the combination of activation signals that contribute to neutrophil-mediated tissue damage during chlamydial infection in the genital

Citation McQueen BE, Kollipara A, Gyorke CE, Andrews CW, Jr, Ezzell A, Darville T, Nagarajan UM. 2021. Reduced uterine tissue damage during *Chlamydia muridarum* infection in TREM-1,3-deficient mice. *Infect Immun* 89: e00072-21. <https://doi.org/10.1128/IAI.00072-21>.

Editor Craig R. Roy, Yale University School of Medicine

Copyright © 2021 American Society for Microbiology. All Rights Reserved.

Address correspondence to Uma M. Nagarajan, nagaraja@email.unc.edu.

Received 5 February 2021

Returned for modification 23 March 2021

Accepted 1 June 2021

Accepted manuscript posted online 14 June 2021

Published 16 September 2021

tract remains unclear. A recently described set of receptors, known as triggering receptors expressed on myeloid cells (TREM), has been discovered to modulate myeloid cell activation. TREM-1 is found primarily on monocytes and neutrophils and can independently activate these cells or synergize with Toll-like receptor activation (13–15). TREM-1 is an Ig-like receptor that associates with DNAX activation protein of 12 (DAP-12) to initiate downstream activation of phosphatidylinositol 3-kinase (PI3K) and extracellular signal-regulated kinase (ERK) (16). There are multiple reports of potential ligands for TREM-1 (17–19), which can bind to TREM-1 and result in NF- κ B and nuclear factor of activated T cells (NFAT) activation, causing proinflammatory cytokine/chemokine release, production of reactive oxygen species (ROS), and degranulation (reviewed in reference 20).

Studies using the intracellular pathogens *Leishmania major*, influenza virus, and lymphocytic choriomeningitis virus (LCMV) have demonstrated that TREM-1 deficiency results in reduced disease, thus improving overall outcome (21, 22). Conversely, during extracellular infections with pathogens such as *Klebsiella pneumoniae* and *Pseudomonas aeruginosa*, TREM-1 or TREM-1,3 deficiency led to increased pathogen loads and poor outcomes (23, 24), likely as a result of an impaired innate immune response. In an *Escherichia coli* sepsis model, TREM-1 blockade increased mouse survival by reducing the host's systemic proinflammatory response (14). TREM-1,3 expression also contributed to neutrophil TeM in the murine lung during *P. aeruginosa* infection (24). Together, these findings demonstrate an important role for TREM-1,3 in neutrophil proinflammatory activation and TeM during pathogenesis.

Our lab recently discovered that the TREM-1 signaling pathway is one of the top 10 gene transcriptional pathways upregulated in the whole blood of *C. trachomatis*-infected women with endometritis (25). To address the hypothesis that TREM-1 contributes to genital tract pathology during chlamydial infection, we infected mice deficient for TREM-1,3 (*trem1,3*^{-/-}) with *Chlamydia muridarum* in the genital tract and determined infection course, immune cell recruitment, and endpoint pathology in uterine horns and oviducts. We show that TREM-1 is exclusively expressed on myeloid cells in the genital tracts of infected mice and that loss of TREM-1,3 reduces uterine horn pathology but not oviduct pathology. TREM-1,3 was not essential for clearing chlamydial infection, as infection burden and course in *trem1,3*^{-/-} mice mirrored those in wild-type (WT) mice. Though there was no reduction in the incidence of hydrosalpinx at day 45 postinfection, *trem1,3*^{-/-} mice had a significantly reduced incidence of hydrometra. At 7 days postinfection, we observed that *trem1,3*^{-/-} mice had a reduced number of uterine glands containing polymorphonuclear cells (PMNs), and reduced neutrophil transmigration into the uterine horn accompanied with increased levels of granulocyte colony-stimulating factor (G-CSF). We also observed reduced epithelial erosion 21 days postinfection in *trem1,3*^{-/-} mice. Together, our data indicate a contributory role for TREM-1,3 in neutrophil TeM, luminal epithelial erosion, and hydrometra in mouse uteri during *C. muridarum* infection.

RESULTS

TREM-1 is predominantly expressed on neutrophils in the female mouse genital tract during chlamydial infection. TREM-1 is expressed at high levels on monocytes and neutrophils, but it is also expressed at low levels on T cells and mucosal lung epithelial cells (reviewed in reference 26). To determine the cell types that express TREM-1 in the mouse female genital tract during infection, we infected mice with *C. muridarum*, excised the uterine horns 7 days postinfection to generate single-cell suspensions, and determined surface expression of TREM-1 on multiple cell types by flow cytometry. TREM-1 was not detected on cells that did not express the leukocyte marker CD45, which includes stromal and epithelial cells. In CD45⁺ cells, TREM-1 was not expressed on nonmyeloid cells (CD11b⁻) but was detected on one-third of myeloid cells (CD11b⁺). While a small percentage of monocytes (CD11b⁺ Ly6C⁺ Ly6G⁻) expressed TREM-1, the majority of neutrophils (CD11b⁺ Ly6C⁺ Ly6G⁺) expressed TREM-1

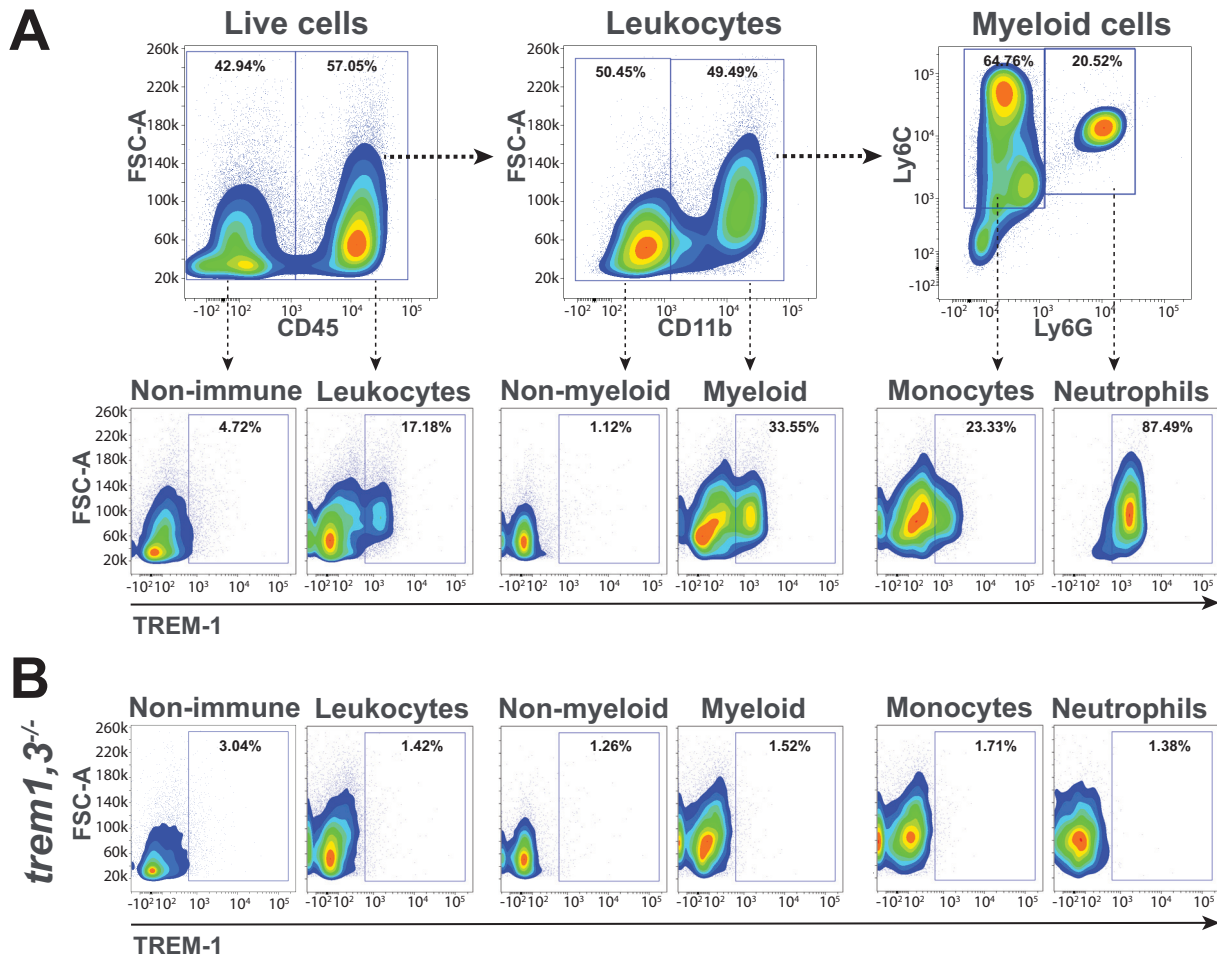


FIG 1 TREM-1 is expressed on myeloid cells in the genital tract during *C. muridarum* infection. C57BL/6J WT ($n=5$) and *trem1,3*^{-/-} ($n=4$) mice were infected with 3×10^5 IFU of *C. muridarum*, and genital tracts were harvested 7 days later. Uterine horn cell suspensions were analyzed for TREM-1 expression in hematopoietic and nonhematopoietic cells by flow cytometry. Representative plots of live-cell subtypes for WT (A) and *trem1,3*^{-/-} mice (B) from one of two experiments are shown. All gates were drawn using appropriate FMO plots.

(Fig. 1A). As expected, myeloid cells from *trem1,3*^{-/-} mice lacked TREM-1 surface expression (Fig. 1B).

TREM-1,3 contributes to pathology in the uterine horns but not the oviducts.

TREM-1 activation of neutrophils leads to ROS production and degranulation (27, 28), which can impact chlamydial growth and tissue pathology. To determine the contribution of TREM-1 to chlamydial pathogenesis, we used a mouse strain in which *trem3* was deleted with *trem1* (24). *trem3* is a pseudogene in humans, shares high sequence homology with *trem1*, and lies adjacent to *trem1* on the genome (29). Further, both TREM-1 and TREM-3 activate shared signaling pathways (29, 30), suggesting overlapping functions. As such, both *trem1* and *trem3* were deleted to mimic a human response (24). WT and *trem1,3*^{-/-} mice were infected with *C. muridarum*, and cervico-vaginal swabs were obtained at intervals over 45 days and assessed for chlamydial DNA by quantitative PCR (qPCR). We observed no difference in chlamydial burden or infection kinetics over a 45-day period in the *trem1,3*^{-/-} mice compared to WT mice (Fig. 2A). At 45 days postinfection, mice were sacrificed, and genital tracts were assessed for gross pathology. Mice deficient in TREM-1,3 had an incidence of hydrosalpinx similar to that of wild-type mice (Fig. 2B and C). Chlamydial infection commonly results in cystic dilatation in the uteri of mice, in which glands are swollen and filled with fluid (31–33), a phenomenon termed hydrometra. Although *trem1,3*^{-/-} mice had numbers of oviducts exhibiting hydrosalpinx, similar to those of WT mice, they

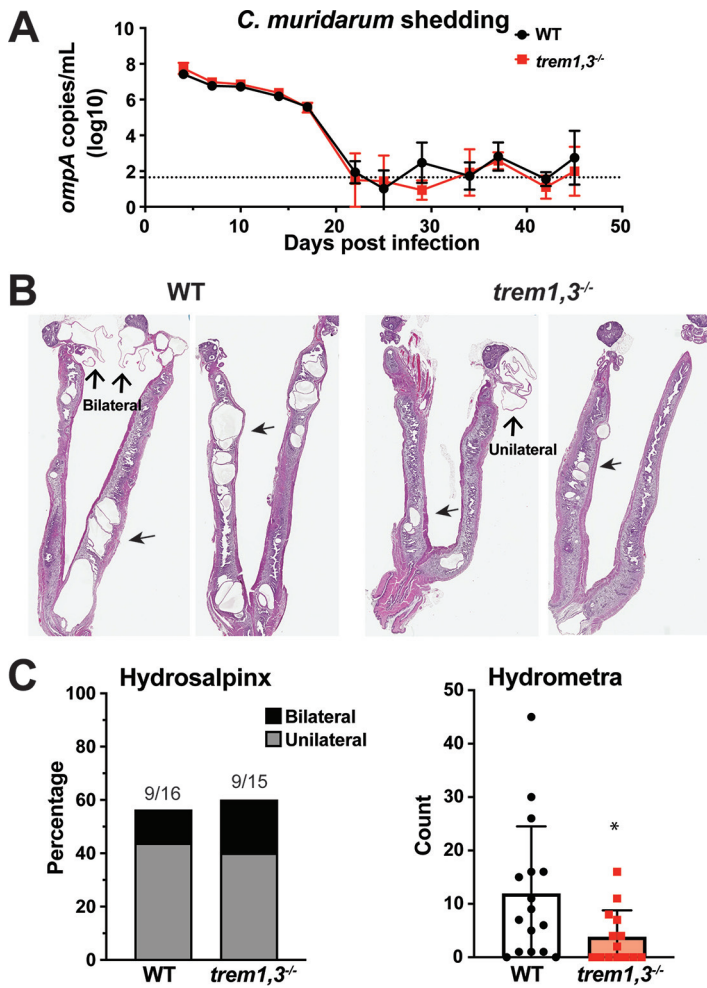


FIG 2 *trem1,3^{-/-}* mice had reduced incidence of hydrometra. (A) C57BL/6J WT ($n=5$) and *trem1,3^{-/-}* ($n=4$) mice were infected with 3×10^5 IFU *C. muridarum*. Chlamydial shedding was determined from vaginal swabs taken at the indicated days postinfection and quantified by qPCR using standard curve measuring copy numbers for the chlamydial MOMP gene. Data are means \pm standard errors of the means (SEM) and are representative of 3 experiments. (B) H&E staining of histological sections of genital tracts from 2 representative mice from each group 45 days postinfection. Arrows indicate hydrosalpinx (open arrows) and hydrometra (solid arrows). Numbers of oviducts exhibiting hydrosalpinx and glands in the uteri exhibiting hydrometra were quantified in each mouse, and data from 3 experiments were combined. $n=16$ (WT) and 15 (*trem1,3^{-/-}*) (C). Hydrosalpinx incidence was classified as unilateral (one side) or bilateral (both sides). Data are means \pm SD. *, $P < 0.05$.

developed significantly fewer glands exhibiting hydrometra in their uteri (Fig. 2B and C). Therefore, TREM-1,3 signaling contributes to uterine pathology during infection.

TREM-1,3 contributes to neutrophil transepithelial migration. To investigate the possible contributing factors that led to hydrometra, we assessed histological sections from 7 days postinfection. We found the presence of PMNs in the uterine horn glands in WT mice, which was less frequent in *trem1,3^{-/-}* mice (Fig. 3). However, we were unable to accurately quantify glandular size and number of PMNs present due to limitations of single-plane histological sectioning. Therefore, we sought to determine if TREM-1,3 deficiency altered neutrophil infiltration during *Chlamydia* infection in the uterine horns. We observed similar bacterial loads and frequencies of immune cell infiltrates, including monocytes and neutrophils, in single-cell suspensions of whole uterine horn tissues at 7 days postinfection (see Fig. S1A and B in the supplemental material). Immunohistochemical staining for neutrophils revealed prominent infiltrates in the lumens of both WT and *trem1,3^{-/-}* mice 7 days postinfection. However, increased densities of neutrophils were observed at the basal surface of the uterine horn luminal epithelium in *trem1,3^{-/-}* mice compared to WT

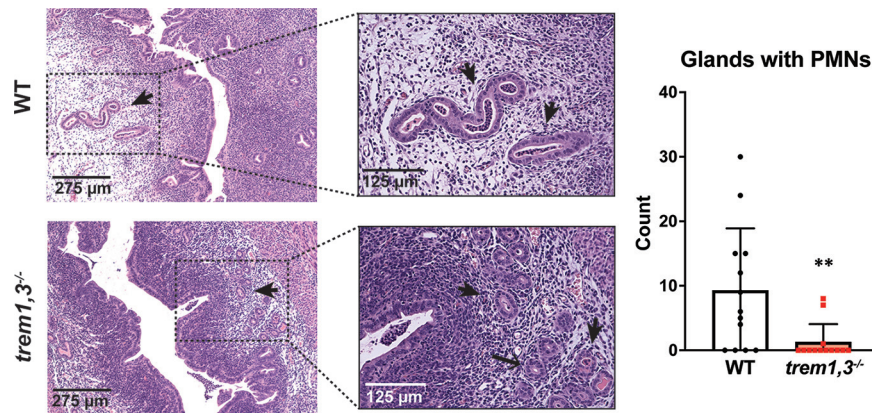


FIG 3 *trem1,3*^{-/-} mice had reduced number of uterine horn glands with polymorphonuclear cell presence. C57BL/6J WT and *trem1,3*^{-/-} mice were infected with 3×10^5 IFU *C. muridarum*, and genital tracts were harvested 7 days postinfection. Representative H&E staining of histological sections of uterine horn glands from WT and *trem1,3*^{-/-} mice with (solid arrows) and without (open arrows) PMNs. The glands in the uterine horns containing PMNs were counted in each mouse. Data are means \pm SD. $n = 13$ from 3 independent experiments. **, $P < 0.01$.

mice (Fig. 4A), suggesting a reduction in neutrophil TeM in the absence of TREM-1,3. Indeed, histological scoring at 7 and 21 days postinfection in the uterine lumen of *trem1,3*^{-/-} mice revealed a reduced presence of PMNs (Fig. 4B).

To calculate the percentage of total neutrophils that had migrated into the lumen, we collected uterine horn lavage fluid, prepared cell suspensions from uterine tissues after lavage, and analyzed them by flow cytometry. Lavage fluid from both WT and *trem1,3*^{-/-} mice contained large numbers of neutrophils. However, the fraction of total tissue neutrophils (Ly6C⁺ Ly6G⁺) that migrated to the lumen was reduced in *trem1,3*^{-/-} mice compared to WT (Fig. 4C), revealing TREM-1,3's contribution to neutrophil TeM in infected uteri. We found no difference in the fractions of total tissue monocytes (Ly6C⁺ Ly6G⁻) in uterine lumens between *trem1,3*^{-/-} and WT mice (data not shown). Interestingly, despite similar neutrophil recruitment to the uterine horns between WT and *trem1,3*^{-/-} mice and a reduced infiltration of neutrophils in the lumen of *trem1,3*^{-/-} mice, at 7 days postinfection we observed increased G-CSF protein in whole-uterine-tissue homogenates (Fig. 4D). However, we observed no difference in CXCL1 (KC) or CXCL2 (MIP-2) proteins in the uterine horn homogenates between WT and *trem1,3*^{-/-} mice (Fig. S1C), while IL-1 β , TNF- α , and CCL2 (MCP-1) levels were below the level of detection in WT and *trem1,3*^{-/-} mice (data not shown). Together, our data indicate an association between reduced hydrometra and glandular PMN infiltration, which could be the result of reduced PMN TeM.

***trem1,3*^{-/-} mice have reduced epithelial erosions in the uterine horns.** Neutrophils in the lumen can cause damage to epithelial barriers by releasing toxic granules (34). To determine if the defect in neutrophil TeM would impact epithelial erosion, WT and *trem1,3*^{-/-} mice were evaluated for epithelial erosion by histological scoring at 7, 21, and 45 days postinfection. Mice deficient for TREM-1,3 had slightly reduced erosion scores 7 days postinfection and significantly reduced erosion scores 21 days postinfection (Fig. 5). At 45 days postinfection, despite WT mice having more extensive hydrometra than *trem1,3*^{-/-} mice, both WT and *trem1,3*^{-/-} mice were able to repair their uterine epithelium (Fig. 5). Histological scoring revealed no difference in the extent of dilatation or lymphocyte infiltration in the uterine horns (Fig. S2) at 7, 21, and 45 days postinfection. We also observed no difference in PMN or mononuclear cell infiltration, dilatation, or epithelial erosion in the oviducts (Fig. S3). These data suggest that TREM-1,3 contributes to epithelial erosion in the uterine horns during infection.

DISCUSSION

While *Chlamydia* infections can be cured via antibiotic therapy, upper-genital-tract damage as a result of an overly robust host immune response can be irreversible.

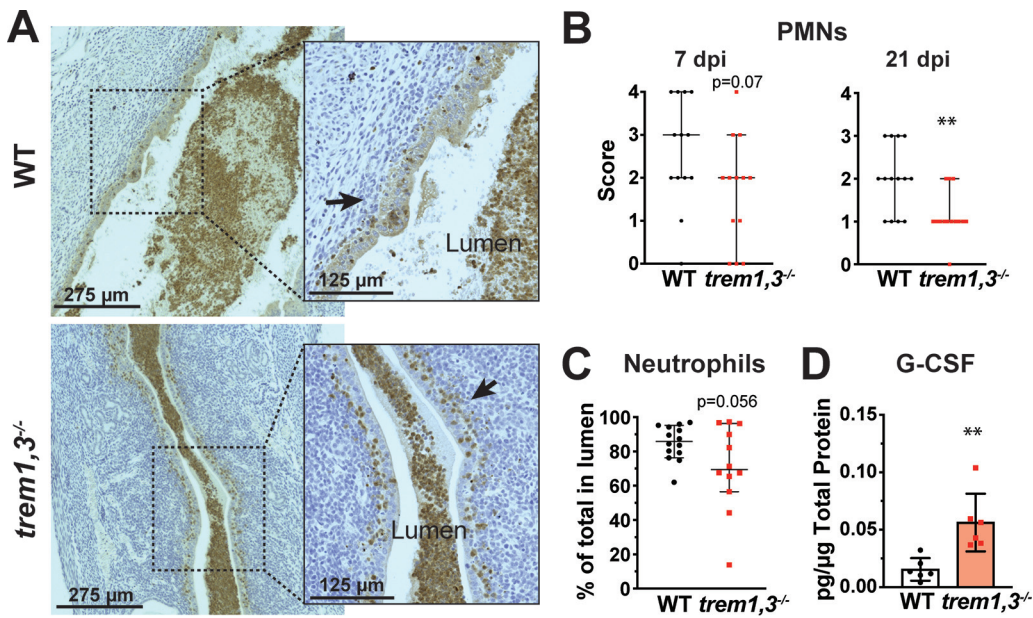


FIG 4 *trem1,3*^{-/-} mice had reduced neutrophils in the uterine horn lumen. Infected C57BL/6J WT and *trem1,3*^{-/-} mice were harvested 7 and 21 days postinfection. (A) Immunohistochemical staining with antineutrophil antibody of representative histological sections 7 days postinfection. Neutrophils are highlighted in brown using DAB as the detection chromogen, and solid arrows indicate the basal portion of the uterine horn luminal epithelium. (B) Histological sectioning of the uterine horns was scored for polymorphonuclear cell (neutrophil) infiltration into the lumen 7 days postinfection (dpi). At 7 dpi, *n* = 13 for 3 experiments combined. At 21 dpi, *n* = 14 for 2 experiments combined. **, *P* < 0.01. (C) Lavage fluid was collected from excised uterine horns, and neutrophils in lavage fluid and tissues after lavage were quantified by flow cytometry. The percent total neutrophils in the lumen is the percentage of the ratio of lavage neutrophils to lavage and tissue neutrophils. *n* = 14 (WT) and 12 (*trem1,3*^{-/-}). Data are means ± SEM. (D) In an independent experiment, tissue homogenates were prepared from uterine horns excised from mice 7 days postinfection and analyzed for G-CSF by Luminex. *n* = 6. **, *P* < 0.01.

Understanding the molecular and cellular mechanisms that induce tissue damaging inflammation would aid development of adjunctive therapies to prevent sequelae. Neutrophils are strongly associated with chronic tissue damage in the female reproductive tract during chlamydial infection. In this study, we investigated the contribution of TREM-1,3, an activation receptor highly expressed on neutrophils, to chlamydial pathogenesis. Using the mouse model of genital *Chlamydia* infection, we demonstrated that TREM-1,3 does not contribute to infection control but contributes to neutrophil-induced pathology in the uterine horns.

The contribution of TREM-1,3 to chlamydial immunopathology but not to infection clearance is consistent with other infection models which also rely on a T cell response to combat infection. Specifically, mice deficient in TREM-1 expression were able to control *Leishmania major* and influenza virus infections similarly to WT mice while having reduced immunopathology from infiltrating neutrophils (21). Similarly, TREM-1-deficient mice infected with LCMV displayed reduced hepatic injury that is commonly associated with infiltrating neutrophils (22). The lack of an effect of TREM-1,3 deficiency on chlamydial burden is not surprising, given that *Chlamydia* spp. are obligately intracellular pathogens and the primary mechanism for control of infection is adaptive Th1 T cells (35–38), while neutrophils are dispensable in primary infection and play only a supportive role in secondary infections (6, 38, 39).

In our infection model, we observed a reduction in neutrophil-associated immunopathology in the uterus during chlamydial infection, indicating TREM-1,3's ability to enhance the tissue-damaging inflammatory response. However, we did not observe any reduction in hydrosalpinx occurrence in TREM-1,3-deficient mice, suggesting that either TREM-1,3's role is confined to the uteri or that alternate receptors which contribute to oviduct pathology, such as Toll-like receptor 2 (TLR2) (40), tumor necrosis factor receptor (TNF-R) (41), and/or interleukin 1 receptor (IL-1R) (42), are too damaging in

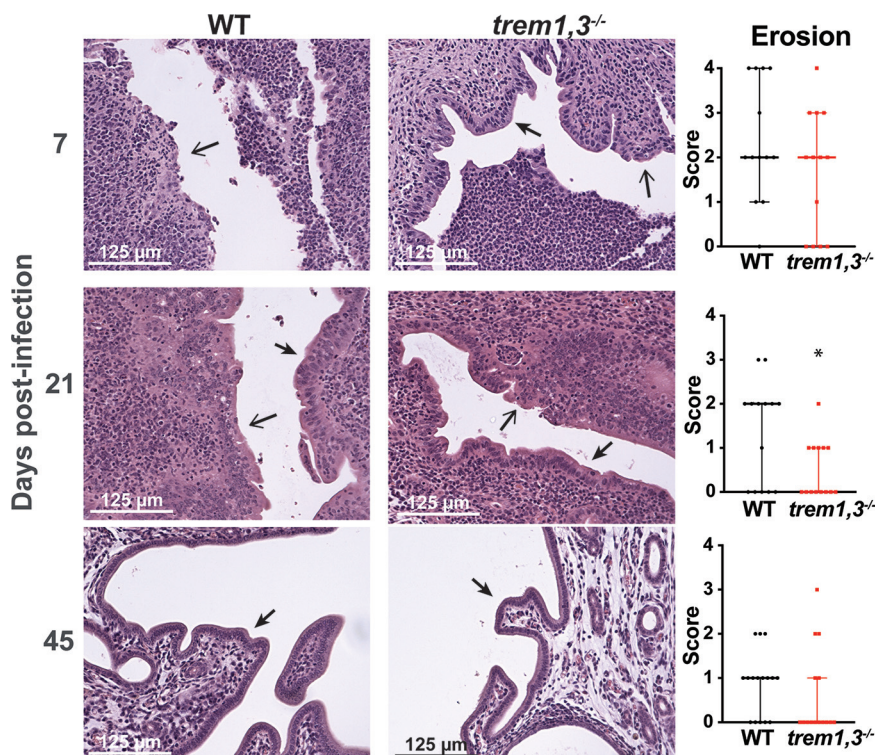


FIG 5 *trem1,3*^{-/-} mice had reduced uterine horn epithelial erosions. Genital tracts from infected C57BL/6J WT and *trem1,3*^{-/-} mice were harvested 7, 21, and 45 days postinfection. Representative H&E staining of the uterine horn luminal epithelium from histological sections of WT and *trem1,3*^{-/-} mice. Solid arrows indicate intact epithelium, and open arrows indicate eroded and/or disrupted epithelium. Semiquantitative scoring of epithelial erosion was performed on all sections. Sections were scored from 1 to 4 as described in Materials and Methods. At day 7 postinfection, $n=12$ (WT) and 13 (*trem1,3*^{-/-}) for three combined experiments. At day 21 postinfection, $n=14$ for two combined experiments. At day 45 postinfection, $n=16$ (WT) and 15 (*trem1,3*^{-/-}) for three combined experiments. *, $P < 0.05$.

the oviduct to allow a contribution of TREM-1,3 to be observed. Alternatively, the fragile nature of the oviducts compared to the uteri could also make the tissue more susceptible to neutrophil-induced damage, masking the contribution of TREM-1,3 to TeM. We speculate that since TREM-1,3 synergizes with TLRs to enhance myeloid cell activation (27), blockade of TREM-1,3 in combination with TLR2 could enhance the protective effects of TLR2 deficiency and reveal a contributory role for TREM-1,3 in the oviducts.

Studies have reported reduced neutrophil migration in the absence of TREM-1 signaling (21, 43), and a study by Klesney-Tait et al. (24) linked TREM-1,3 to neutrophil TeM in the lung, which was essential for murine host defense against *P. aeruginosa* infection. Mice deficient in TREM-1,3 had decreased infiltration of neutrophils into the bronchiolar airspace, which resulted in increased bacterial burden and mortality. They further showed the deficit in neutrophil migration was likely a result of ROS production (28). Our results showed some reduction in neutrophil TeM into the uterine horn lumen but no effect on neutrophil or lymphocyte tissue infiltration or rate of bacterial clearance. The comparatively reduced effect that we observed of TREM-1,3 deficiency on neutrophil transmigration suggests that additional neutrophil receptors are engaged during chlamydial infection to elicit transmigration. Additionally, loss of epithelial polarity, cytotoxicity, and barrier disruption induced by chlamydial infection (44) surely provides access for neutrophils to migrate into the lumen in the absence of TREM-1,3 activation.

Interestingly, we observed increased levels of G-CSF in uterine homogenates from *trem1,3*^{-/-} mice. G-CSF binds to its receptor (G-CSFR) on neutrophils. Therefore, we speculate that reduced neutrophils in the uterine lumen of *trem1,3*^{-/-} mice result in

increased unbound detectable G-CSF. In support of this, in arthritis and LPS-induced lung injury models, neutrophil recruitment is followed by a reduction in detectable G-CSF (45, 46). Although effects of TREM-1,3 on TeM were mild in our model, our data revealed a reduction in uterine horn epithelial erosion in TREM-1,3-deficient mice during infection. However, the mechanism by which TREM-1,3 promotes epithelial erosion is unclear. We suspect that it is a result of reduced neutrophil TeM or neutrophil activation, and both should be considered in further investigations.

It is well established that the formation and function of uterine glands are critical to support egg implantation and fetal growth by providing the necessary nutrients for development (reviewed in reference 47). A common characteristic of genital chlamydial infections in mice is hydrometra, an accumulation of fluid that enlarges uterine glands, which do not repair themselves. This chronic pathology has been shown to cause obstruction and prevent efficient uterine contraction, which aids in fertility in mice (48–50). Here, we report a reduction in the number of uterine glands containing PMNs early during infection and a reduction in the occurrence of hydrometra in the absence of TREM-1,3. The exact mechanism of uterine hydrometra is not clear. It could be a result of neutrophil inflammation and damage that causes excessive epithelial and inflammatory cell debris in the glands, leading to blockade that causes eventual fluid accumulation. Epithelial cell death could release damage-associated molecular patterns (DAMPs) and pathogen-associated molecular patterns (PAMPs), which lead to further immune activation in uterine glands. Our data from *trem1,3*^{-/-} mice suggest that TREM-dependent epithelial erosion resulting from neutrophil TeM likely contributes to hydrometra. However, a direct link between epithelial erosion and hydrometra requires further investigation. In humans, histopathological analysis of *Chlamydia*-induced endometritis is associated with increased PMNs in the endometrial glands (51, 52), making hydrometra in mice analogous to pathology observed in humans.

Given the strong association between chlamydial infections and endometritis (53), more efforts are needed to mitigate immunopathology incurred in the endometrium during infection. A common feature of chlamydial infection in women is neutrophil infiltration in the lumen of glands in the endometrium (52, 54), similar to what is seen in the mouse model. Since TREM-1 has a role in tissue damage in the uteri of mice, this receptor may be a suitable therapeutic target to reduce endometrial inflammation during chlamydial infection without compromising host defense responses important in infection resolution. Further, identification and blockade of other neutrophil innate inflammatory receptors in combination with TREM-1 blockade may reduce excessive damage in the upper genital tract during chlamydial infection.

MATERIALS AND METHODS

Mice. Age-matched wild-type C57BL/6J mice were purchased from The Jackson Laboratory (Bar Harbor, ME; 000664) and acclimated to the animal facility at the University of North Carolina at Chapel Hill (UNC-CH) for at least 7 days prior to experiments. For this study, we obtained mice deficient in *trem1* and *trem3* from Julia Klesney-Tait at the University of Iowa Carver College of Medicine (24). Genetic deletion of *trem1,3* was confirmed by genomic PCR with the primers TCTCTCCATCTATGCATCCACCC (F1), TCCCAAGAGCAGGCACAAGA (F2), and TCTTCCGCTGATTGGTTCA (R) as previously described (24). All mice were housed at the UNC-CH animal facility in a pathogen-free environment, and studies were approved by the IACUC.

***Chlamydia muridarum* infection.** *Chlamydia muridarum* strain Nigg stocks were propagated and titrated in L929 monolayers as previously described (55). Stocks were stored in sucrose-sodium phosphate-glutamic acid (SPG) buffer at 80°C until use. Eight- to 10-week-old mice were administered 2.5 mg Depo-Provera (medroxyprogesterone acetate [Upjohn]) in 100 μ l sterile phosphate-buffered saline (PBS) subcutaneously 7 to 10 days prior to infection to induce anestrus. Mice were anesthetized intraperitoneally with 10 μ l/gram weight of sodium pentobarbital (5 mg/ml) in sterile PBS and infected intravaginally with 3×10^5 inclusion-forming units (IFU) in 20 μ l SPG buffer. At the indicated time points, chlamydial shedding was assayed with cervicovaginal swabs of each mouse that were rotated 10 times. Swabs were collected in 1 ml SPG buffer, and DNA was extracted using a Quick-DNA miniprep kit (Zymo D3024). The amount of chlamydial DNA in extracts was quantified by qPCR using primers against *ompA* (encoding major outer membrane protein [MOMP]) as previously described (56).

Flow cytometry. Uterine horns were excised from mice postmortem and processed for flow cytometry analysis. For uterine horn lavages, uterine horns were cut 2 mm above the cervix and below the oviducts. Two hundred microliters of Hanks balanced salt solution (HBSS) (without Ca or Mg) with 5% fetal

bovine serum (FBS) was carefully pipetted through each uterine horn with a 200- μ l pipet tip and collected. The remaining tissue and uterine horns that had not been subjected to lavage were processed as previously described (57). Briefly, single-cell suspensions of tissues were obtained by mincing of tissue and digestion with collagenase for 60 min at 37°C. Digested tissues were filtered through a 70- μ m filter followed by a 40- μ m filter to obtain single-cell suspensions. Cells were stained with Zombie UV live/dead stain (BioLegend 423107) diluted 1:500 in PBS. Cells were washed with cell stain buffer (BioLegend 420201) and resuspend in Fc block (BD 553142). Cells were stained using the following antibodies with conjugated fluorophores: anti-CD45–peridinin chlorophyll protein (PerCP)–Cy5.5 (BD clone 30-F11), anti-CD11b–allophycocyanin (APC) (BioLegend clone M1/70), anti-Ly6G–fluorescein isothiocyanate (FITC) (BioLegend clone IA8), anti-Ly6C–BV605 (BioLegend clone HK1.4), anti-F4/80–phycoerythrin (PE)–Dazzle (BioLegend clone BM8), anti-TREM-1–PE (R&D FAB1187P), anti-CD3–APC/Cy7 (BioLegend clone 17A2), and/or anti-CD8 α –PE/Cy7 (BioLegend clone 53-6.7). Gating for immune cells was performed as previously described using appropriate fluorescence minus one (FMO) controls (57). Cells were washed 3 times in cell stain buffer and fixed in 2% formaldehyde. Cells were analyzed on an LSR II flow cytometer (BD) at the UNC Flow Cytometry Core, and data were analyzed using Cytobank (58).

Cytokine expression. After preparation of single-cell suspensions for flow cytometry, 1/20 of each cell suspension was isolated and diluted 1:2. After a freeze-thaw cycle to lyse cells, supernatants were collected, and total protein was quantified using a bicinchoninic acid (BCA) assay kit (Pierce 23225). Supernatants were assayed for cytokines using a Milliplex MAP mouse cytokine/chemokine magnetic bead panel (Millipore MCYTOMAG-70K) containing beads with antibodies against mouse G-CSF, IL-1 β , CXCL1 (KC), CXCL2 (MIP-2), CCL2 (MCP-1), and TNF- α following the manufacturer's protocol. Analysis was performed using a Bio-Rad MAGPIX multiplex reader with Bio-Plex Manager MP software (Bio-Rad). Cytokine concentrations were normalized to total protein levels in each sample. Samples that fell below the level of detection were reduced to half of the lower level of detection.

Immunohistochemistry. Genital tracts of mice were removed postmortem and placed in 10% formalin in PBS for 24 h. Tissues were rinsed with PBS for 24 h and embedded in paraffin. Sections of the genital tract were cut longitudinally 4 μ m thick and stained with hematoxylin and eosin (H&E). The method for counting uterine glands exhibiting hydrometra was previously described (33). Histological scoring was performed using a previously described semiquantitative 4-tier rating system (59). The endocervix, uterine horns, oviducts, and mesosalpinx were evaluated for polymorphonuclear cells (PMNs), mononuclear cells, plasma cells, dilatation, chronic inflammation, and fibrosis. To detect neutrophils, paraffin-embedded sections were deparaffinized and rehydrated using a series of graded alcohols. Heat-induced epitope retrieval was performed using pH 6.0 buffer (Thermo TA-135-HBL), after which endogenous peroxidase activity was quenched with 3% hydrogen peroxide. Sections were blocked in 10% normal goat serum for 1 h and then incubated overnight at 4°C with rat anti-neutrophil antibody (Abcam AB2557) diluted 1:100. Sections were then incubated in biotinylated goat anti-rat IgG (Jackson 112-065-167) diluted 1:500 for 1 h at room temperature. Signal was amplified with a Vectastain Elite ABC-HRP kit (Vector Laboratories PK-6100), per the manufacturer's instructions and detected using the chromogen DAB (3,3'-diaminobenzidine) (Thermo TA-125-QHDX). Finally, sections were counterstained with hematoxylin (Thermo 6765003), dehydrated with a series of graded ethanols, cleared with xylene, and coverslipped with DPX mounting medium (EMS 13512).

Statistical analysis. For chlamydial shedding data from multiple time points, experiments were performed twice. All statistical analysis was performed using GraphPad's Prism 9.0 software. Statistical significance was determined using two-way analysis of variance (ANOVA) with Sidak's multiple comparison. Statistical significance for hydrometra incidence was determined using a *t* test with Welch's correction. Statistical analysis for chlamydial IFU in tissue was performed using nonparametric Mann-Whitney test. Cell counts, measured by flow cytometry, were determined for each cell type, and each cell type was calculated as a percentage of the total live-cell population. Statistical analysis performed on cell type quantification was performed using two-way ANOVA with Sidak's multiple-comparison test. For histological scoring, statistical significance was determined using a nonparametric Mann-Whitney test. *n* values for each experiment are included in the figure legends.

SUPPLEMENTAL MATERIAL

Supplemental material is available online only.

SUPPLEMENTAL FILE 1, PDF file, 1 MB.

ACKNOWLEDGMENTS

We thank Julia Klesney-Tait at the University of Iowa for providing *trem1,3*^{-/-} mice.

The study was fully funded through Translational Team Science Award (UNC School of Medicine and NC TRACS) and partly funded by NIAID NIH R01 AI067678 to UN. B.E.M. was supported by STI T32 grant AI007001. The UNC Flow Cytometry Core Facility is supported in part by a P30 CA016086 Cancer Center Core Support grant to the UNC Lineberger Comprehensive Cancer Center. Research reported in this publication was supported in part by the North Carolina Biotech Center Institutional Support grant 2017-IDG-1025 and by the National Institutes of Health 1UM2AI30836-01. The UNC Translational Pathology Laboratory is supported in part by grants from the NCI

(5P30CA016086-42), NIH (U54-CA156733), NIEHS (5 P30 ES010126-17), UCRF, and NCBT (2015-IDG-1007). The UNC Center for Gastrointestinal Biology and Disease Histology Core Facility is supported by a grant from the NIH (P30 DK 034987).

The content is solely the responsibility of the authors and does not necessarily represent the official views of the National Institutes of Health.

We declare no conflict of interest.

B.E.M. designed and performed experiments under advisement of U.M.N. and T.D. Flow cytometry experiments were designed and conducted by B.E.M., C.E.G., and A.K. Histological scoring was performed by C.W.A. A.E. developed and performed neutrophil staining of mouse tissue sections and wrote the corresponding methods section. B.E.M. wrote the manuscript, with revisions performed by B.E.M., T.D., and U.M.N.

REFERENCES

- Centers for Disease Control and Prevention. 2016. Sexually transmitted disease surveillance 2015. Department of Health and Human Services, Atlanta, GA.
- O'Connell CM, Ferone ME. 2016. Chlamydia trachomatis genital infections. *Microb Cell* 3:390–403. <https://doi.org/10.15698/mic2016.09.525>.
- Brunham RC, Paavonen J. 2020. Reproductive system infections in women: lower genital tract syndromes. *Pathog Dis* 78:ftaa022. <https://doi.org/10.1093/femspd/ftaa022>.
- Brunham RC, Paavonen J. 2020. Reproductive system infections in women: upper genital tract, fetal, neonatal and infant syndromes. *Pathog Dis* 78:ftaa023. <https://doi.org/10.1093/femspd/ftaa023>.
- Lee HY, Schripsema JH, Sigar IM, Murray CM, Lacy SR, Ramsey KH. 2010. A link between neutrophils and chronic disease manifestations of Chlamydia muridarum urogenital infection of mice. *FEMS Immunol Med Microbiol* 59:108–116. <https://doi.org/10.1111/j.1574-695X.2010.00668.x>.
- Lijek RS, Helble JD, Olive AJ, Seiger KW, Starnbach MN. 2018. Pathology after Chlamydia trachomatis infection is driven by nonprotective immune cells that are distinct from protective populations. *Proc Natl Acad Sci U S A* 115:2216–2221. <https://doi.org/10.1073/pnas.1711356115>.
- Imtiaz MT, Distelhorst JT, Schripsema JH, Sigar IM, Kasimos JN, Lacy SR, Ramsey KH. 2007. A role for matrix metalloproteinase-9 in pathogenesis of urogenital Chlamydia muridarum infection in mice. *Microbes Infect* 9:1561–1566. <https://doi.org/10.1016/j.micinf.2007.08.010>.
- Wang SZ, Xu H, Wraith A, Bowden JJ, Alpers JH, Forsyth KD. 1998. Neutrophils induce damage to respiratory epithelial cells infected with respiratory syncytial virus. *Eur Respir J* 12:612–618. <https://doi.org/10.1183/09031936.98.12030612>.
- Venaille TJ, Ryan G, Robinson BW. 1998. Epithelial cell damage is induced by neutrophil-derived, not pseudomonas-derived, proteases in cystic fibrosis sputum. *Respir Med* 92:233–240. [https://doi.org/10.1016/S0954-6111\(98\)90101-9](https://doi.org/10.1016/S0954-6111(98)90101-9).
- Zemans RL, Briones N, Campbell M, McClendon J, Young SK, Suzuki T, Yang IV, De Langhe S, Reynolds SD, Mason RJ, Kahn M, Henson PM, Colgan SP, Downey GP. 2011. Neutrophil transmigration triggers repair of the lung epithelium via beta-catenin signaling. *Proc Natl Acad Sci U S A* 108:15990–15995. <https://doi.org/10.1073/pnas.1110144108>.
- Rank RG, Whittimore J, Bowlin AK, Dessus-Babus S, Wyrick PB. 2008. Chlamydiae and polymorphonuclear leukocytes: unlikely allies in the spread of chlamydial infection. *FEMS Immunol Med Microbiol* 54:104–113. <https://doi.org/10.1111/j.1574-695X.2008.00459.x>.
- Futosi K, Fodor S, Mocsai A. 2013. Neutrophil cell surface receptors and their intracellular signal transduction pathways. *Int Immunopharmacol* 17:638–650. <https://doi.org/10.1016/j.intimp.2013.06.034>.
- Bouchon A, Dietrich J, Colonna M. 2000. Cutting edge: inflammatory responses can be triggered by TREM-1, a novel receptor expressed on neutrophils and monocytes. *J Immunol* 164:4991–4995. <https://doi.org/10.4049/jimmunol.164.10.4991>.
- Bouchon A, Facchetti F, Weigand MA, Colonna M. 2001. TREM-1 amplifies inflammation and is a crucial mediator of septic shock. *Nature* 410:1103–1107. <https://doi.org/10.1038/35074114>.
- Arts RJ, Joosten LA, Dinarello CA, Kullberg BJ, van der Meer JW, Netea MG. 2011. TREM-1 interaction with the LPS/TLR4 receptor complex. *Eur Cytokine Netw* 22:11–14. <https://doi.org/10.1684/ecn.2011.0274>.
- Tessarz AS, Cerwenka A. 2008. The TREM-1/DAP12 pathway. *Immunol Lett* 116:111–116. <https://doi.org/10.1016/j.imlet.2007.11.021>.
- Haselmayer P, Grosse-Hovest L, von Landenberg P, Schild H, Radsak MP. 2007. TREM-1 ligand expression on platelets enhances neutrophil activation. *Blood* 110:1029–1035. <https://doi.org/10.1182/blood-2007-01-069195>.
- Read CB, Kuijper JL, Hjorth SA, Heipel MD, Tang X, Fleetwood AJ, Dantzer JL, Grell SN, Kastrop J, Wang C, Brandt CS, Hansen AJ, Wagtmann NR, Xu W, Stenicke VW. 2015. Cutting edge: identification of neutrophil PGLYRP1 as a ligand for TREM-1. *J Immunol* 194:1417–1421. <https://doi.org/10.4049/jimmunol.1402303>.
- Wu J, Li J, Salcedo R, Mivechi NF, Trinchieri G, Horuzsko A. 2012. The proinflammatory myeloid cell receptor TREM-1 controls Kupffer cell activation and development of hepatocellular carcinoma. *Cancer Res* 72:3977–3986. <https://doi.org/10.1158/0008-5472.CAN-12-0938>.
- Tammaro A, Derive M, Gibot S, Leemans JC, Florquin S, Dessing MC. 2017. TREM-1 and its potential ligands in non-infectious diseases: from biology to clinical perspectives. *Pharmacol Ther* 177:81–95. <https://doi.org/10.1016/j.pharmthera.2017.02.043>.
- Weber B, Schuster S, Zysset D, Rihs S, Dickgreber N, Schurch C, Riether C, Siegrist M, Schneider C, Pawelski H, Gurzeler U, Ziltener P, Genitsch V, Tacchini-Cottier F, Ochsenbein A, Hofstetter W, Kopf M, Kaufmann T, Oxenius A, Reith W, Saurer L, Mueller C. 2014. TREM-1 deficiency can attenuate disease severity without affecting pathogen clearance. *PLoS Pathog* 10:e1003900. <https://doi.org/10.1371/journal.ppat.1003900>.
- Kozik JH, Trautmann T, Carambia A, Preti M, Lutgehetmann M, Krech T, Wiegand C, Heeren J, Herkel J. 2016. Attenuated viral hepatitis in Trem1^{-/-} mice is associated with reduced inflammatory activity of neutrophils. *Sci Rep* 6:28556. <https://doi.org/10.1038/srep28556>.
- Lin YT, Tseng KY, Yeh YC, Yang FC, Fung CP, Chen NJ. 2014. TREM-1 promotes survival during Klebsiella pneumoniae liver abscess in mice. *Infect Immun* 82:1335–1342. <https://doi.org/10.1128/IAI.01347-13>.
- Klesney-Tait J, Keck K, Li X, Gilfillan S, Otero K, Baruah S, Meyerholz DK, Varga SM, Knudson CJ, Moninger TO, Moreland J, Zabner J, Colonna M. 2013. Transepithelial migration of neutrophils into the lung requires TREM-1. *J Clin Invest* 123:138–149. <https://doi.org/10.1172/JCI64181>.
- Zheng X, O'Connell CM, Zhong W, Poston TB, Wiesenfeld HC, Hillier SL, Trent M, Gaydos C, Tseng G, Taylor BD, Darville T. 2018. Gene expression signatures can aid diagnosis of sexually transmitted infection-induced endometritis in women. *Front Cell Infect Microbiol* 8:307. <https://doi.org/10.3389/fcimb.2018.00307>.
- Roe K, Gibot S, Verma S. 2014. Triggering receptor expressed on myeloid cells-1 (TREM-1): a new player in antiviral immunity? *Front Microbiol* 5:627. <https://doi.org/10.3389/fmicb.2014.00627>.
- Radsak MP, Salih HR, Rammensee HG, Schild H. 2004. Triggering receptor expressed on myeloid cells-1 in neutrophil inflammatory responses: differential regulation of activation and survival. *J Immunol* 172:4956–4963. <https://doi.org/10.4049/jimmunol.172.8.4956>.
- Baruah S, Murthy S, Keck K, Galvan I, Prichard A, Allen LH, Farrelly M, Klesney-Tait J. 2019. TREM-1 regulates neutrophil chemotaxis by promoting NOX-dependent superoxide production. *J Leukoc Biol* 105:1195–1207. <https://doi.org/10.1002/JLB.3VMA0918-375R>.
- Chung DH, Seaman WE, Daws MR. 2002. Characterization of TREM-3, an activating receptor on mouse macrophages: definition of a family of single Ig domain receptors on mouse chromosome 17. *Eur J Immunol* 32:59–66. [https://doi.org/10.1002/1521-4141\(200201\)32:1<59::AID-IMMU59>3.0.CO;2-U](https://doi.org/10.1002/1521-4141(200201)32:1<59::AID-IMMU59>3.0.CO;2-U).

30. Chen LC, Laskin JD, Gordon MK, Laskin DL. 2008. Regulation of TREM expression in hepatic macrophages and endothelial cells during acute endotoxemia. *Exp Mol Pathol* 84:145–155. <https://doi.org/10.1016/j.yexmp.2007.11.004>.
31. Nguyen N, Olsen AW, Lorenzen E, Andersen P, Hvid M, Follmann F, Dietrich J. 2020. Parenteral vaccination protects against transcervical infection with *Chlamydia trachomatis* and generate tissue-resident T cells post-challenge. *NPJ Vaccines* 5:7. <https://doi.org/10.1038/s41541-020-0157-x>.
32. Gondek DC, Olive AJ, Stary G, Starnbach MN. 2012. CD4+ T cells are necessary and sufficient to confer protection against *Chlamydia trachomatis* infection in the murine upper genital tract. *J Immunol* 189:2441–2449. <https://doi.org/10.4049/jimmunol.1103032>.
33. Sun X, Yang Z, Zhang H, Dai J, Chen J, Tang L, Rippentrop S, Xue M, Zhong G, Wu G. 2015. *Chlamydia muridarum* induction of glandular duct dilation in mice. *Infect Immun* 83:2327–2337. <https://doi.org/10.1128/IAI.00154-15>.
34. Brazil JC, Parkos CA. 2016. Pathobiology of neutrophil-epithelial interactions. *Immunol Rev* 273:94–111. <https://doi.org/10.1111/imr.12446>.
35. Naglak EK, Morrison SG, Morrison RP. 2016. IFN γ is required for optimal antibody-mediated immunity against genital *Chlamydia* infection. *Infect Immun* 84:3232–3242. <https://doi.org/10.1128/IAI.00749-16>.
36. Zhang Y, Wang H, Ren J, Tang X, Jing Y, Xing D, Zhao G, Yao Z, Yang X, Bai H. 2012. IL-17A synergizes with IFN- γ to upregulate iNOS and NO production and inhibit chlamydial growth. *PLoS One* 7:e39214. <https://doi.org/10.1371/journal.pone.0039214>.
37. Vicetti Miguel RD, Quispe Calla NE, Pavelko SD, Cherpes TL. 2016. Intra-vaginal *Chlamydia trachomatis* challenge infection elicits TH1 and TH17 immune responses in mice that promote pathogen clearance and genital tract damage. *PLoS One* 11:e0162445. <https://doi.org/10.1371/journal.pone.0162445>.
38. Dockterman J, Coers J. 2021. Immunopathogenesis of genital *Chlamydia* infection: insights from mouse models. *Pathog Dis* 79:ftab012. <https://doi.org/10.1093/femspd/ftab012>.
39. Naglak EK, Morrison SG, Morrison RP. 2017. Neutrophils are central to antibody-mediated protection against genital *Chlamydia*. *Infect Immun* 85:e00409-17. <https://doi.org/10.1128/IAI.00409-17>.
40. Darville T, O'Neill JM, Andrews CW, Jr, Nagarajan UM, Stahl L, Ojcius DM. 2003. Toll-like receptor-2, but not Toll-like receptor-4, is essential for development of oviduct pathology in chlamydial genital tract infection. *J Immunol* 171:6187–6197. <https://doi.org/10.4049/jimmunol.171.11.6187>.
41. Dong X, Liu Y, Chang X, Lei L, Zhong G. 2014. Signaling via tumor necrosis factor receptor 1 but not Toll-like receptor 2 contributes significantly to hydrosalpinx development following *Chlamydia muridarum* infection. *Infect Immun* 82:1833–1839. <https://doi.org/10.1128/IAI.01668-13>.
42. Nagarajan UM, Sikes JD, Yeruva L, Prantner D. 2012. Significant role of IL-1 signaling, but limited role of inflammasome activation, in oviduct pathology during *Chlamydia muridarum* genital infection. *J Immunol* 188:2866–2875. <https://doi.org/10.4049/jimmunol.1103461>.
43. Yang C, Chen B, Zhao J, Lin L, Han L, Pan S, Fu L, Jin M, Chen H, Zhang A. 2015. TREM-1 signaling promotes host defense during the early stage of infection with highly pathogenic *Streptococcus suis*. *Infect Immun* 83:3293–3301. <https://doi.org/10.1128/IAI.00440-15>.
44. Kessler M, Zielecki J, Thieck O, Mollenkopf HJ, Fotopoulou C, Meyer TF. 2012. *Chlamydia trachomatis* disturbs epithelial tissue homeostasis in fallopian tubes via paracrine Wnt signaling. *Am J Pathol* 180:186–198. <https://doi.org/10.1016/j.ajpath.2011.09.015>.
45. Campbell IK, Leong D, Edwards KM, Rayzman V, Ng M, Goldberg GL, Wilson NJ, Scalzo-Inguanti K, Mackenzie-Kludas C, Lawlor KE, Wicks IP, Brown LE, Baz Morelli A, Panousis C, Wilson MJ, Nash AD, McKenzie BS, Andrews AE. 2016. Therapeutic targeting of the G-CSF receptor reduces neutrophil trafficking and joint inflammation in antibody-mediated inflammatory arthritis. *J Immunol* 197:4392–4402. <https://doi.org/10.4049/jimmunol.1600121>.
46. Banuelos J, Cao Y, Shin SC, Bochner BS, Avila P, Li S, Jiang X, Lingen MW, Schleimer RP, Lu NZ. 2017. Granulocyte colony-stimulating factor blockade enables dexamethasone to inhibit lipopolysaccharide-induced murine lung neutrophils. *PLoS One* 12:e0177884. <https://doi.org/10.1371/journal.pone.0177884>.
47. Cooke PS, Spencer TE, Bartol FF, Hayashi K. 2013. Uterine glands: development, function and experimental model systems. *Mol Hum Reprod* 19:547–558. <https://doi.org/10.1093/molehr/gat031>.
48. Kunstly I, Matthiesen T, Gartner K, Maess J, Heimann W. 1982. Post-mating non-infectious hydrometra in BALB/c:Bom mice. *Lab Anim* 16:51–55. <https://doi.org/10.1258/002367782780908922>.
49. Pal S, Peterson EM, de la Maza LM. 2001. Susceptibility of mice to vaginal infection with *Chlamydia trachomatis* mouse pneumonitis is dependent on the age of the animal. *Infect Immun* 69:5203–5206. <https://doi.org/10.1128/IAI.69.8.5203-5206.2001>.
50. Antonson P, Matic M, Portwood N, Kuiper RV, Bryzgalova G, Gao H, Windahl SH, Humire P, Ohlsson C, Berggren PO, Gustafsson JA, Dahlman-Wright K. 2014. aP2-Cre-mediated inactivation of estrogen receptor alpha causes hydrometra. *PLoS One* 9:e85581. <https://doi.org/10.1371/journal.pone.0085581>.
51. Paavonen J, Aine R, Teisala K, Heinonen PK, Punnonen R, Lehtinen M, Miettinen A, Gronroos P. 1985. Chlamydial endometritis. *J Clin Pathol* 38:726–732. <https://doi.org/10.1136/jcp.38.7.726>.
52. Kiviat NB, Wolner-Hanssen P, Eschenbach DA, Wasserheit JN, Paavonen JA, Bell TA, Critchlow CW, Stamm WE, Moore DE, Holmes KK. 1990. Endometrial histopathology in patients with culture-proved upper genital tract infection and laparoscopically diagnosed acute salpingitis. *Am J Surg Pathol* 14:167–175. <https://doi.org/10.1097/00000478-199002000-00008>.
53. Eckert LO, Hawes SE, Wolner-Hanssen PK, Kiviat NB, Wasserheit JN, Paavonen JA, Eschenbach DA, Holmes KK. 2002. Endometritis: the clinical-pathologic syndrome. *Am J Obstet Gynecol* 186:690–695. <https://doi.org/10.1067/mob.2002.121728>.
54. Paavonen J, Teisala K, Heinonen PK, Aine R, Miettinen A, Lehtinen M, Gronroos P. 1985. Endometritis and acute salpingitis associated with *Chlamydia trachomatis* and herpes simplex virus type two. *Obstet Gynecol* 65:288–291.
55. Prantner D, Darville T, Sikes JD, Andrews CW, Jr, Brade H, Rank RG, Nagarajan UM. 2009. Critical role for interleukin-1 β (IL-1 β) during *Chlamydia muridarum* genital infection and bacterial replication-independent secretion of IL-1 β in mouse macrophages. *Infect Immun* 77:5334–5346. <https://doi.org/10.1128/IAI.00883-09>.
56. Allen J, Gyorke CE, Tripathy MK, Zhang Y, Lovett A, Montgomery SA, Nagarajan UM. 2019. Caspase-11 contributes to oviduct pathology during genital *Chlamydia* infection in mice. *Infect Immun* 87:e00262-19. <https://doi.org/10.1128/IAI.00262-19>.
57. Gyorke CE, Kollipara A, Allen J, Zhang Y, Ezzell JA, Darville T, Montgomery SA, Nagarajan UM. 2020. IL-1 α is essential for oviduct pathology during genital chlamydial infection in mice. *J Immunol* 205:3037–3049. <https://doi.org/10.4049/jimmunol.2000600>.
58. Kotecha N, Krutzik PO, Irish JM. 2010. Web-based analysis and publication of flow cytometry experiments. *Curr Protoc Cytom Chapter 10:Unit10.17*. <https://doi.org/10.1002/0471142956.cy1017s53>.
59. Darville T, Andrews CW, Jr, Sikes JD, Fraley PL, Rank RG. 2001. Early local cytokine profiles in strains of mice with different outcomes from chlamydial genital tract infection. *Infect Immun* 69:3556–3561. <https://doi.org/10.1128/IAI.69.6.3556-3561.2001>.